

Targeted Whole-Cell Recordings in the Mammalian Brain In Vivo

Neurotechnique

Troy W. Margrie,^{1,2,*} Axel H. Meyer,³
Antonio Caputi,³ Hannah Monyer,³
Mazahir T. Hasan,¹ Andreas T. Schaefer,¹
Winfried Denk,¹ and Michael Brecht¹

¹Max-Planck Institute for Medical Research
Jahnstrasse 29
69120 Heidelberg
Germany

²The Wolfson Institute for Biomedical Research
Department of Physiology
University College London
Gower Street
London WC1E 6BT
United Kingdom

³Department of Clinical Neurobiology
University Hospital of Neurology
Neuenheimer Feld 364
69120 Heidelberg
Germany

Summary

While electrophysiological recordings from visually identified cell bodies or dendrites are routinely performed in cell culture and acute brain slice preparations, targeted recordings from the mammalian nervous system are currently not possible *in vivo*. The “blind” approach that is used instead is somewhat random and largely limited to common neuronal cell types. This approach prohibits recordings from, for example, molecularly defined and/or disrupted populations of neurons. Here we describe a method, which we call TPTP (two-photon targeted patching), that uses two-photon imaging to guide *in vivo* whole-cell recordings to individual, genetically labeled cortical neurons. We apply this technique to obtain recordings from genetically manipulated, parvalbumin-EGFP-positive interneurons in the somatosensory cortex. We find that both spontaneous and sensory-evoked activity patterns involve the synchronized discharge of electrically coupled interneurons. TPTP applied *in vivo* will therefore provide new insights into the molecular control of neuronal function at the systems level.

Introduction

Optical microscopy techniques have revolutionized our approach to studying neuronal activity in brain tissue (Masters, 1996; Denk and Svoboda, 1997; Helmchen et al., 2001). Most of the neuronal single-cell imaging studies carried out to date have focused on acute (Pettit et al., 1995) or cultured brain slice preparations (Okabe et al., 1999; Shi et al., 1999). More recently, fluorescence microscopy has permitted recordings *in vitro* to be targeted toward neurons belonging to specific populations

that were genetically modified, for example, to express biological fluorophores including green fluorescent protein (GFP), often used as a cellular indicator of successful gene manipulation (Pines, 1995; Takada et al., 1997; Fischer et al., 1998; Mainen et al., 1999; Lundstrom, 2001; Shi et al., 2001). Although the immediate cellular environment of the neurons in these preparations is thought to remain intact, functional long-range connections are lost, the modulatory environment is compromised, and stimulation by sensory input is (with the exception of the retina) not possible. Despite significant progress toward understanding the molecular basis of synaptic transmission, it has therefore not been possible to examine the physiological role of cell type-specific proteins in orchestrating neuronal responses *in vivo*.

While blind *in vivo* intracellular recording techniques have provided invaluable information regarding synaptic and dendritic integration, input-output relations, and receptive fields of single cells (Eccles, 1957; Nelson et al., 1994; Jagadeesh et al., 1993; Zhu and Connors, 1999; Kamondi et al., 1998; Stern et al., 2001; Margrie and Schaefer, 2003), one limiting factor in the acquisition of such information is that the type of the recorded cell is often not apparent. This makes it difficult to tailor the experimental protocol to a particular cell type and often limits the interpretability of the data obtained, especially if no post hoc histological analysis is available. A further limitation of blind recording techniques is that experiments cannot be directed toward examining differences across molecularly identified or spatially diffuse classes of neurons (e.g., parvalbumin-positive versus calretinin-positive interneurons), and it is impossible to specifically sample cells that have been genetically modified.

Two-photon excitation (Denk et al., 1990) has permitted fluorescence detection deep within neural tissue (more than 0.5 mm) in the intact brain (Denk et al., 1994; Svoboda et al., 1997; Chen et al., 2000; Oheim et al., 2001; Charpak et al., 2001). Two-photon microscopy has been combined with blind intracellular recordings to investigate the spatial and temporal properties of $[Ca^{2+}]$ signals in neuronal dendritic compartments *in vivo* (Svoboda et al., 1997, 1999; Helmchen et al., 1999). The two-photon targeted patching (TPTP) technique described here, which involves the combination of two-photon imaging and whole-cell recordings, enables intracellular recordings from molecularly identifiable cell types. In this case, we have successfully targeted cells expressing EGFP driven by a specific promoter introduced by the BAC technique. This approach allows electrophysiological characterization of specific neurons and investigation into their role in network function. We demonstrate the power of TPTP by targeting whole-cell recordings from parvalbumin-positive interneurons in the mouse somatosensory cortex, where we find support for the hypothesis that electrical coupling between interneurons is involved in the patterning of sensory-evoked cortical activity.

*Correspondence: t.margrie@ucl.ac.uk

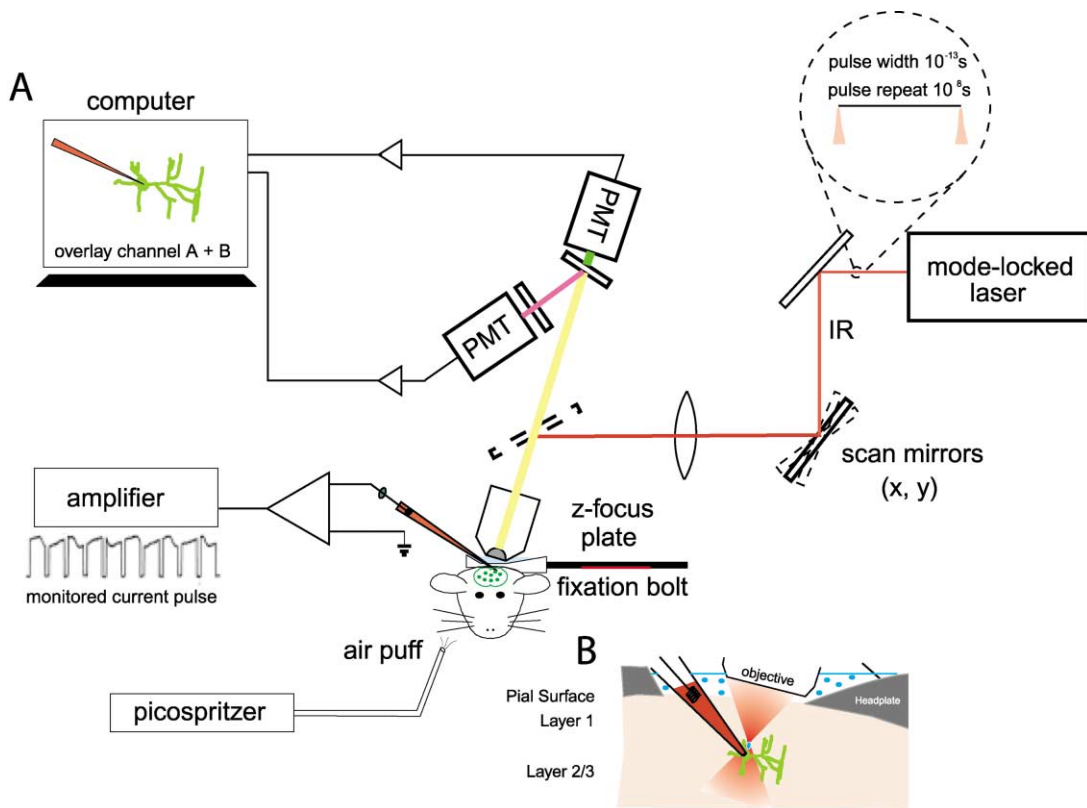


Figure 1. Targeted Whole-Cell Recordings from EGFP Neurons In Vivo Using Visual and Electrical Guidance

(A) Emitted light was detected by two photomultipliers (PMTs) and recorded separately. An overlay of the two fluorescence signals was performed using a table that assigned a user-defined color to every combination of PMT intensities. During the final approach, pipette resistance was used to detect contact between pipette and cell membrane. Below, an example trace is shown of the change in electrode resistance at heartbeat frequency observed when the pipette is in contact with neuronal membranes.

(B) Under high magnification, water immersion conditions were established by loading the imaging window of the headplate chamber (which was fixed to the cranium) with Ringer's solution.

Results

Procedure for Obtaining Targeted Whole-Cell Recordings In Vivo

Optical Requirements for TPTP

Since our goal was to direct patch-clamp recordings from EGFP-labeled neurons in vivo, it was necessary to visualize the pipette using the two-photon microscope. To achieve this, we used conventional patch pipettes (4–7 M Ω resistance) with tip diameters of approximately 1.5 μ m with internal solution containing the fluorescent dye Alexa 594, which can be clearly distinguished due to its different emission spectrum from GFP when imaging with the two-photon excitation microscope (Figure 1A). Initially, using low-power magnification (4 \times objective) under video guidance, the patch pipettes were coarsely guided onto the cortex to approximately the center of the field of view, which was positioned over the barrel cortex. The low-power objective was then replaced by a water immersion objective (Nikon 40 \times 0.8NA; Figure 1B). Now the dye-filled patch pipette and the EGFP cells were imaged simultaneously with two detection channels using the custom-built two-photon microscope, schematically shown in Figure 1. For successful navigation of the patch pipette toward the EGFP-labeled cells,

it was very helpful to overlay the two channels using a false color combination look-up table (Figures 1 and 2).

Considerations

Two-photon excitation fluorescence has previously been used to detect calcium transients in cortical neurons in vivo (Svoboda et al., 1997, 1999; Helmchen et al., 1999), which provides a quantitative measure of the spatiotemporal properties of dendritic function. Thus, there would be considerable advantages to using internal solutions containing ion-sensitive indicators for targeted recordings. We therefore attempted to target patch recordings with pipettes containing various calcium indicators, in particular calcium orange (which can be spectrally separated from GFP). However, since positive pressure is required to keep the tip of the pipette free from contamination, the background fluorescence signal (indicator fluorescence increases due to the extracellular calcium in the cerebrospinal fluid) was almost always too high to visualize the pipette tip. This problem was diminished by the use of the orange to red fluorescent Alexa dye that is insensitive to ionic composition and provides strong visible fluorescence, which contrasts well with the green fluorescence of the EGFP. The problem of background fluorescence was further reduced by (1) applying only relatively small positive

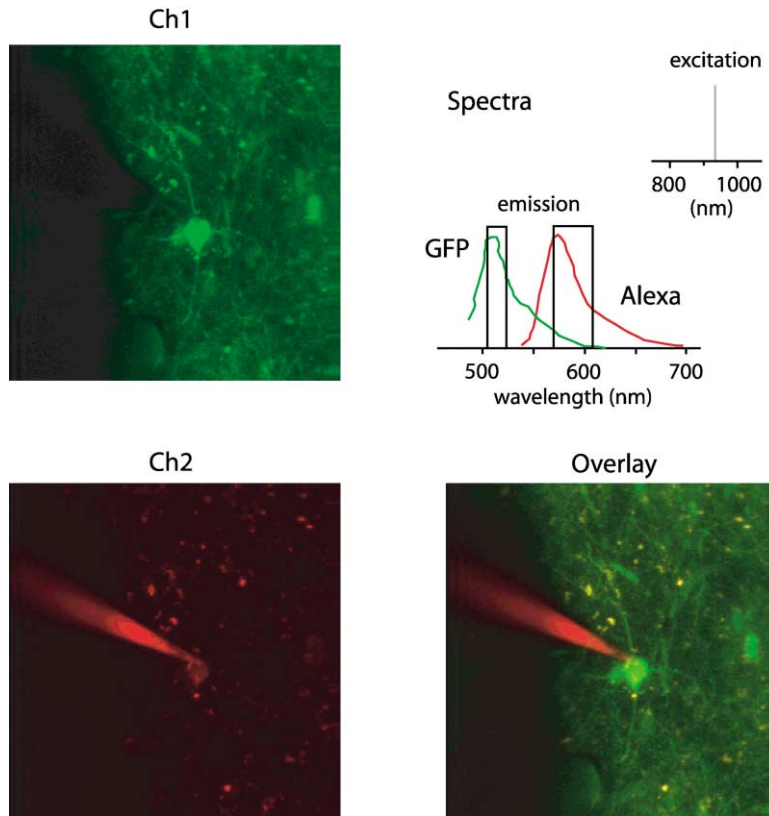


Figure 2. Dual-Channel Two-Photon Imaging

Two-photon scanning microscope image of a parvalbumin-EGFP-expressing interneuron in the mouse barrel cortex. Ch 1: the green channel showing the soma and dendrites of a EGFP-labeled neuron located in Layer 2/3. Ch 2: the patch pipette containing Alexa 594 and the overlay of the two channels. The emission filter for the first PMT (green channel) and the second PMT (red channel) is indicated by the black box. The wavelength of the laser is indicated on the right by the gray line.

pressures (10–20 mbar) during the final approach toward the cell, (2) a fast navigation of the patch pipette toward the cell, and (3) a change of recording sites after a few unsuccessful penetrations.

Pipette Navigation and Target Requirements

The pipettes were first lowered into layer 2/3 under low zoom magnification (field of view $\sim 500 \times 500 \mu\text{m}$) fluorescence guidance to track the entry of the pipette through the pia and upper cortical layers. Once the pipette was positioned inside the upper cortical layers, a target cell was chosen. We used two main criteria for cell selection. First, to keep laser intensity to a minimum, we chose a cell with large fluorescence signals. A second consideration was to take into account the amount of lateral movement required to hit a putative target. To minimize potential damage to the cortex caused by lateral movement of the pipette, cells were chosen that were no more than $200 \mu\text{m}$ distant from the trajectory axis. In this way, the integrity of the cortex in the local region could be maintained.

Considerations

When the lateral electrode movements were restricted, tissue damage and the rupture of capillaries or larger blood vessels were almost never observed. The limiting factor of repeated attempts was the increasing background signal caused by residual internal solution. Due to the sufficient density of parv-EGFP neurons, it was not necessary to choose a target cell prior to pipette entry into the brain. Choosing a trajectory before entry into the brain, which will be needed to target very sparse populations, should be possible by using suitably calibrated micromanipulators.

Obtaining Whole-Cell Recordings by Combined Visual and Electric Guidance

Once the target cell was chosen, the pipette was directed toward the cell using continuous triangular micromanipulator movements in the XYZ planes. Even under the most favorable conditions, the two-photon fluorescence image does not provide the finely resolved details of cell membrane and pipette tip that is used to guide seal formation by differential interference contrast microscopy for in vitro preparations. Therefore, it was essential to use, in addition to visual guidance, the electrical signal to detect when the patch electrode came in contact with the cell membrane (Figure 1A; Margrie et al., 2002). Once the pipette was positioned in the immediate vicinity of the target cell (5 to $10 \mu\text{m}$ from the cell soma), the fluorescence image was magnified (scan amplitude decreased) so the pipette tip was clearly visible (field of view ranging from $\sim 70 \times 70$ to $30 \times 30 \mu\text{m}$). In voltage clamp when the pipette contacts membranous tissue, the amplitude of the current step in response to the injected voltage is modulated by the heartbeat-associated movement (Margrie et al., 2002). During the final step when the visual and electrical signals were matched, the positive pressure was removed and slight suction was applied to induce Giga-ohm seal formation (Hamill et al., 1981; Margrie et al., 2002).

Considerations

In our initial attempts to target recordings, we employed rather strong illumination levels to ensure an optimal visualization of cell and patch pipette. Under such conditions, we were able to image cell and pipette for prolonged periods and, as judged by the electric signal,

able to bring both cell membranes and pipettes into close contact. However, seal formation between the targeted neuron and the patch pipette was almost never successful under strong illumination. One possible reason for the failure of seal formation could be photo-damage of the targeted neuron or photo-chemical interactions between the laser and the internal solution of the pipette (e.g., Schrader et al., 1998). To minimize those effects, we reduced image resolution and minimized the scanning rate, adjusted the dye concentration in the internal solution to match pipette and cell brightness, and ensured that navigation of the pipette toward the cell was as fast as possible. In addition, a sufficient level of EGFP expression was necessary for successful targeting; in a mouse line with low EGFP expression (only a single copy of the EGFP-containing BAC inserted in the genome), the laser power required for visualization invariably led to tissue damage. We noticed that in our preparation the appearance of laser-induced electric artifacts was a strong predictor of excessive laser power. These artifacts, which are generated by a hitherto unknown mechanism, consist of small (<100 pA) and brief (<0.1 ms) spike-like deflections occurring at kHz rates and occurred predominately at higher magnification levels. We estimated that at the highest magnification levels the maximally tolerable average focal laser intensity is between 1 and 10 mW.

Visual and Physiological Confirmation of Successful Targeting of Layer 2/3 Parvalbumin-Positive Interneurons

Two lines of evidence indicate successful targeting of parvalbumin-positive interneurons. First, in some cases we recorded the fluorescence signals in both the red and green channel to determine whether we successfully recorded from a EGFP-expressing neuron. In all cases a perfect overlay between the washed-in Alexa signal and the EGFP-labeled cell was observed ($n = 5$, Figure 3A). Second, electrophysiological recordings from these cells revealed intrinsic properties identical to those previously described in vitro (Meyer et al., 2002; Galarreta and Hestrin, 2002). We observed fast spiking responses of up to 300 Hz in response to injection of positive current steps (Figure 3B; Galarreta and Hestrin, 2002). These cells discharged APs with fast kinetics (see Table 1) and displayed an average resting membrane voltage of -63 ± 3 mV ($n = 13$). In order to determine the degree of spike frequency adaptation, we measured the average of the last three interspike intervals and divided by the average of the first three interspike intervals. This ratio was calculated from 3–7 sweeps for each cell that discharged ten or more APs in response to a given positive current step (Table 1). Typical of such cortical interneurons (Galarreta and Hestrin, 2002), we found that the targeted recordings showed very little spike adaptation and displayed AHPs of smaller amplitude with fast kinetics compared to regular spiking cortical cells (Figure 3B; Table 1; Mason and Larkman, 1990; Kasper et al., 1994). These targeted recordings, therefore, showed the electrophysiological hallmarks of recordings obtained from parvalbumin-positive interneurons in acute brain slices (Meyer et al., 2002; Galarreta and Hestrin, 2002).

Success Rate of TPTP

In order to establish TPTP, it was necessary to optimize conditions using many experimental preparations (greater than 100). Eventually, however, under optimal conditions, TPTP was used successfully to obtain targeted recordings in 50%–70% of preparations. Under optimal conditions, a targeted whole-cell recording was obtained for one of every five to ten penetrations. Up to 20 penetrations per animal were possible before the optical conditions due to background signals from residual pipette internal fluid prevented successful TPTP. Recordings lasted for 15–60 min, and the quality of recordings (stability of membrane potential, series resistance) was comparable to those of L2/3 interneurons obtained by blind in vivo whole-cell recordings in rat barrel cortex (data not shown).

An Application of TPTP: Spikelet Patterning in Parvalbumin-Positive Interneurons during Spontaneous and Sensory-Evoked Neuronal Activity

The most significant aspect of intracellular recordings in vivo is that sensory-evoked subthreshold and supra-threshold activity can be examined. Although electrical coupling between interneurons in acute brain slice preparations is well documented, there remains no direct evidence that such coupling plays any role in orchestrating sensory-evoked responses. Since parvalbumin-positive interneurons are both chemically and electrically coupled (Figure 4A; Meyer et al., 2002; Galarreta and Hestrin, 2002), we used TPTP to search for evidence of network-related spikelet activity. Such spikelet waveforms typically have amplitudes of less than 5 mV, are biphasic with kinetics comparable to an AP, and are believed to be the product of gap junction-mediated electrical coupling (Watanabe, 1958; Furshpan and Potter, 1959; MacVicar and Dudek, 1981; Taylor and Dudek, 1982; Dermietzel and Spray, 1993; Vigmond et al., 1997; Gibson et al., 1999; Bennett, 2000; Tamas et al., 2000; Hormuzdi et al., 2001; Galarreta and Hestrin, 1999, 2001, 2002). In a subset of cells, we observed ongoing spikelet activity at a frequency of 1.0 ± 0.4 Hz ($n = 3$) that was comparable the mean spontaneous AP rate (0.86 ± 0.3 Hz, $n = 13$; Figures 4A and 4B). Qualitatively, we only observed spikelets when the membrane potential was depolarized. To further investigate the relationship between spikelet occurrence and membrane voltage, we performed a “spikelet-triggered” average of the membrane potential (Figure 4B). The average membrane potential measured preceding the peak of the aligned spikelets by 3 ms was significantly more depolarized (-55 ± 1 mV versus -61 ± 3 mV, $p < 0.05$, $n = 31$ events; Figure 4B) than that preceding the spikelet by 200 ms. This indicates that spikelet activity occurs preferentially when the recorded cell is at more depolarized potentials.

We next investigated sensory-evoked spikelet discharge in these cells. Air-puff stimulation of the whisker array could evoke spikelets that occurred preferentially at depolarized potentials and with precise temporal locking to the stimulus (delay of 78 ± 9 ms; $n = 13$ responses, $n = 3$ cells; Figure 4C). Although even at depolarized membrane potential spikelet activity was

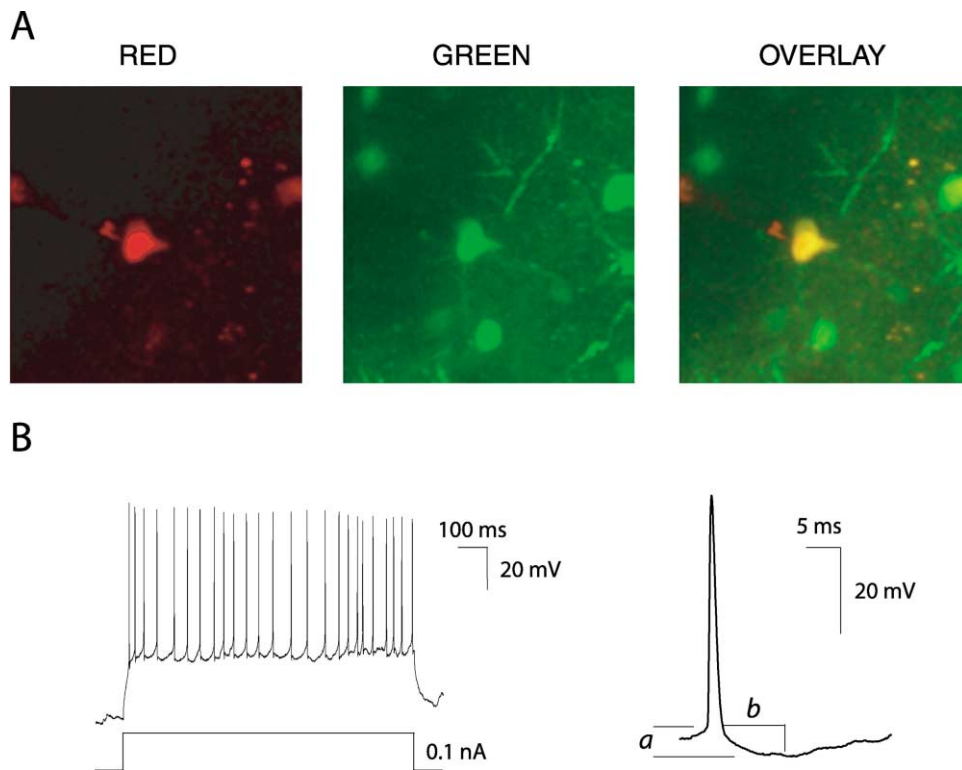


Figure 3. Visual and Electrophysiological Confirmation of Successful TPTP

(A) Projected images of the red and green channels recorded 3 min after break-in. An overlay of the two channels shows that the cell recorded from (red) is the same as the targeted parvalbumin-EGFP cell (green).

(B) The fast firing profile of the targeted cell is shown at left. On the right is an example trace illustrating the kinetics of the spike's afterhyperpolarization (AHP) (*a* and *b* refer to the amplitude and time to peaks measurement used for quantification of AHP properties).

evoked only occasionally by sensory stimulation (approximately 10% of trials, $n = 3$ cells), the same sensory stimulus *never* triggered a spikelet if the prestimulus membrane potential was not sufficiently depolarized (-58 ± 3 mV, $n = 13$ versus -65 ± 1 mV, $n = 127$ trials, measured 5 ms prior to stimulus onset, $n = 3$ cells; Figure 4C). In contrast to spikelets observed in ongoing activity, sensory-evoked spikelets were followed by a hyperpolarization. Such hyperpolarizations were larger in amplitude and had a faster rise time when the evoked reponse contained spikelets (Figures 4B and 4C; 6.1 ± 1.5 mV versus 3.6 ± 0.8 mV, slope of the 20%–80% rising phase: spikelet 98 ± 17 μ V/ms versus nonspikelet 21 ± 8 μ V/ms; $n = 3$ cells; $p < 0.05$) and a shorter time to peak (126 ± 8 ms versus 167 ± 16 ms; $n = 3$ cells; $p < 0.05$). This suggests that the evoked spikelet and thus electrical coupling is correlated with the synchronization of inhibition in the local interneuron network.

Table 1. Intrinsic Properties of Targeted EGFP-Positive Neurons

Accommodation ratio	1.3 ± 0.2 (8)
Spike half width (ms)	1.2 ± 0.1 (13)
AHP (slow)	
Peak voltage ^a (mV)	7.7 ± 0.4 (13)
Time to peak ^b (ms)	15 ± 2.2 (13)

^aPeak voltages measured with respect to spike threshold.

^bTime to peak measured from the point at which the spike downstroke crossed spike threshold.

Discussion

TPTP relies on combining the unique features of two-photon microscopy, whole-cell recording, and genetic manipulation to express a fluorescent marker protein. The increasing availability of animals with genetically modified and labeled cellular subpopulations promises a wide range of applications for TPTP, which need not be restricted to neurons. Since two-photon microscopy allows a much larger depth penetration than conventional microscopy, targeted recordings are possible to a depth of about 0.5 mm, which comprises more than half of the cortical thickness in a juvenile mouse. In the future, TPTP may be combined with amplifier-based 2-photon imaging, which allows access to the entire cortical thickness (Theer et al., 2003). While we have not yet succeeded in obtaining recordings with calcium indicator in the internal solution, it seems likely that with an appropriate indicator (preferably one with diminishing fluorescence upon calcium exposure to reduce background problems), the combination of calcium recording and targeted patching will be possible.

Targeted patching provides immediate information on the cell's molecular characteristics, morphology, and intrinsic electrical properties. In addition, we can study the cell's sub- and suprathreshold response properties inside the intact brain. The combination of genetic and molecular labeling techniques with electrophysiological indicators of neuron identity, such as antidromic activa-

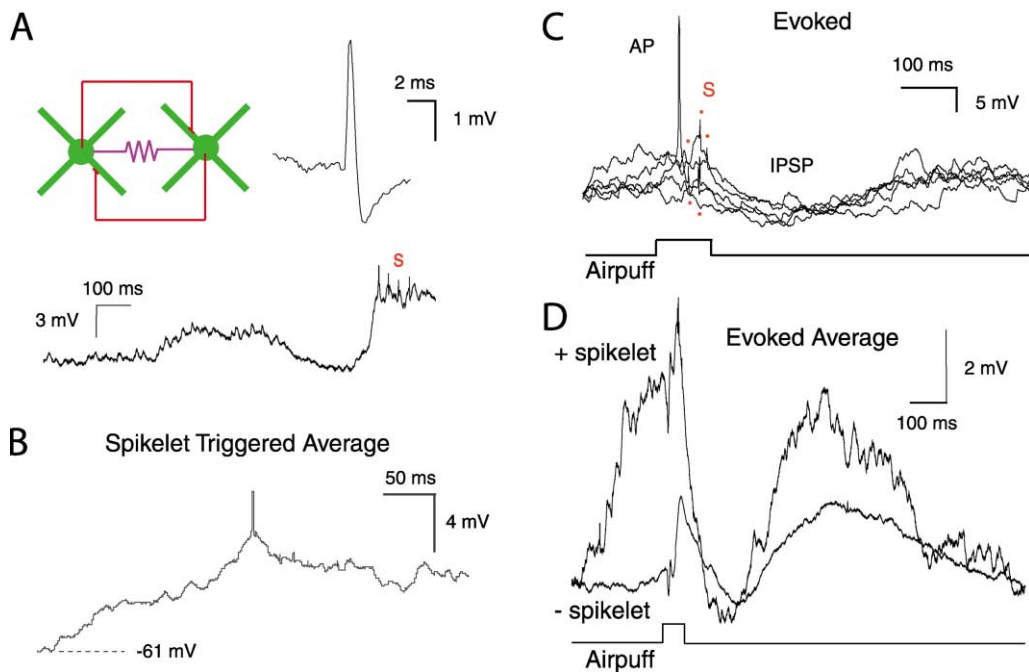


Figure 4. Spontaneous and Evoked Spikelet Activity in Parvalbumin-Positive Interneurons

(A) A cartoon illustrating electrical and chemical transmission between parvalbumin-positive interneurons (axons are shown in red and the electrical coupling is shown schematically in purple). Below is an example trace of individual spontaneously occurring spikelets. An example of such a spikelet is shown in the enlarged panel on the top right.

(B) Spontaneous spikelet-triggered average of the membrane potential showing that spikelet activity occurs preferentially in the depolarized state.

(C) Whisker-evoked spikelet activity and inhibition. Top: example traces from a single cell of evoked spikelet responses ($n = 8$ responses; spikelets are indicated by filled red circles, AP indicates an evoked action potential).

(D) Traces from the same cell showing the average responses of trials containing ($n = 8$) or not containing ($n = 92$) an evoked spikelet.

tion or spiking pattern, will allow a more reliable identification of neurons and possibly the discovery of subtle cellular subclasses.

An important application for TPTP, all but impossible by conventional methods, will be the analysis of the physiological behavior of individual cells that have been transfected (together with the requisite fluorescent marker) by a peptide or protein known or suspected to enhance or suppress physiological function(s). The most obvious application of TPTP is for genetically labeled cells, but other labeling methods that are based on the uptake or transport of synthetic markers or indicators should be equally compatible (Stosiek et al., 2003). This might, for example, permit recordings from a specific subset of cells that project to a certain area of the brain (Kasper et al., 1994).

First Application of TPTP

In order to demonstrate the power of TPTP, we have chosen to investigate the role of electrical coupling in parvalbumin-positive interneurons in the synchronization of sensory-evoked activity. Under general anesthesia, cortical activity is characterized by slow (approximately 1–2 Hz; e.g., Figure 4A) almost rhythmic fluctuations of the membrane potential, which have previously been referred to as up and down states (Steriade et al., 1993; Destexhe and Pare, 1999). Such transients are thought to reflect changes in the amount of network

activity from a relative quiescent period (down state) to episodes of strong synaptic bombardment (up state) (Cowan and Wilson, 1994; Sanchez-Vives and McCormick, 2000; Anderson et al., 2000; Shu et al., 2003). In our experiments, we have used an internal solution that provides a negligible driving force for chloride at the resting membrane potential of these cells. Assuming that there is little or no ongoing network activity during the down state, then the onset of the up state is likely to reflect increased levels of excitation rather than disinhibition onto these cells. Recent *in vitro* work has shown that parvalbumin-positive interneurons are reciprocally coupled by electrical synapses (Galarreta and Hestrin, 2002). There, an action potential in a presynaptic cell resulted in a (electrically postsynaptic) spikelet followed in many cases by a (chemically postsynaptic) GABAergic IPSP (Galarreta and Hestrin, 2002) and well-synchronized inhibition (Deans et al., 2001; Galarreta and Hestrin, 2001). Spikelet activity, therefore, appears to be a specific physiological signature of electrical coupling and promotes synchronization.

Evoked spikelets specifically occurred when a sensory stimulus coincided with an up state and were followed by sharp, fast rising hyperpolarizing potentials. Although we cannot say for certain that the observed postspikelet hyperpolarization was mediated purely by direct GABA-ergic transmission, our data suggest that this hyperpolarization reflects the discharge of an en-

semble of interneurons driven by strong network activity. This sensory-evoked network activity is likely to depend on the synchronization of parvalbumin-positive interneurons that is facilitated by electrical coupling. This view is consistent with both in vitro (Hormuzdi et al., 2001) and in vivo (S. Butovas et al., 2002, Soc. Neurosci., abstract) evidence on the effects of gap junction coupling on the synchronization of inhibition. Using TPTP, we have therefore obtained new insight into the role of electrical coupling in synchronizing cortical inhibition by demonstrating that both spontaneously occurring and sensory-evoked spikelets are linked to particular patterns of network activity (i.e., the up state). We speculate that such synchronized interneuron discharge helps to terminate episodes of strong network excitation.

Experimental Procedures

Surgical Procedures

Mice were anesthetized with urethane (1.2 g/kg) and all pressure points and tissue incisions were infiltrated with lidocaine in accordance with the ethical regulations of the Max-Planck-Gesellschaft. Body temperature was measured via a rectal probe (FHC) and maintained at $37^{\circ}\text{C} \pm 0.2^{\circ}\text{C}$ with a homeothermic blanket (FHC). After clearing the skull of connective tissue, the position of the somatosensory cortex was stereotactically determined and a stainless steel plate shaped to the dorsal surface of the skull was glued on the dorsal surface of the cranium using cyano-acrylate. Following fixation, the headplate was firmly attached to a metal arm mounted on the optical table. A window (3×4 mm) in the headplate allowed access to the somatosensory cortex. Under visual guidance through a dissecting microscope, a craniotomy (1×1 mm) was performed using a high-speed drill (Osada Electric). Following removal of the bone, a small hole was created in the dura to allow access for the patch pipette.

Electrophysiology

As previously described (Margrie et al., 2002) patch pipettes were fabricated using filamented borosilicate glass (OD 2.0 mm, ID 1.5 mm, Hilgenberg, Malsfeld, Germany). The standard intracellular solution was (in mM): K-gluconate 130, Na-gluconate 10, HEPES 10, phosphocreatine 10, MgATP 4, GTP 0.3, NaCl 4, and biocytin 0.3%–1%, Alexa 594 .06 (pH 7.2). The junction potential of +7 mV was corrected for. The surface of the cortex was covered with standard Ringer's solution (in mM): NaCl 125, KCl 2.5, NaHCO_3 25, NaH_2PO_4 1.25, MgCl_2 1, glucose 25, CaCl_2 2. Recordings were amplified using an Axoclamp-2B amplifier (Axon Instruments, Foster City, CA), filtered at 3–10 kHz and digitized at 5–20 kHz (ITC-16; Instrutech, New York, NY) and acquired using HEKA software. For whole-cell recordings, the pipette was directed at the cortex at an angle of approximately 30° to the cortical surface. Statistics given are for mean \pm SEM unless otherwise stated. For whisker stimulation, air puffs (30–60 psi) were delivered via a picospritzer unit (Parker Instrumentation, NH). Air puffs were applied through a pipette tip with a 2 mm opening positioned approximately 1 cm rostro-lateral from the whiskers. The stimulus usually deflected 4–8 whiskers in 2–3 whisker rows by up to 2 mm.

Two-Photon Imaging

We used a custom-built 2-photon microscope to image fluorescence in the intact brain. Fluorescence was generated using 2-photon excitation by a mode-locked Ti-sapphire laser (Coherent Mira, 930 nm, 100 fs, 76 MHz, about 1 W average output power) with a 0.8 NA water-immersion $40\times$ objective (Nikon). Scanning was controlled by custom-written scanning software (Ray Stepnoski, Lucent Technologies, and Michael Müller, MPIfM). A two-channel whole-area detector (using Hamamatsu R6357 photomultipliers) was used to collect emitted light selected by custom interference filters (Chroma Technology, Brattleboro, VT, purchased through AHF, Tübingen, FRG) for monitoring the EGFP (520/BP30) and Alexa

594 (610/BP40) signals. The pixel dwell time was 7.8 μs , and the frame size was 256 pixels \times 256 pixels.

Generation of Transgenic Mice

Generation of the parvalbumin-EGFP mouse has been recently described in detail (Meyer et al., 2002). In these mice approximately 94% of cortical cells show colocalization of EGFP and parvalbumin (Meyer et al., 2002; Blatow et al., 2003). No changes in the transgene expression pattern were observed between the different generations although the intensity of the EGFP signal varied.

Acknowledgments

This work was supported by the Alexander von Humboldt Foundation, the NHMRC of Australia, the Max-Planck-Gesellschaft, the Boehringer Ingelheim Fonds, The European Molecular Biology Organization, and The Wellcome Trust. We thank Nathan Urban for helpful discussions, Bert Sakmann for support, and P. Chadderton and S. Hormuzdi for comments on the manuscript.

Received: January 21, 2003

Revised: June 26, 2003

Accepted: August 12, 2003

Published: September 10, 2003

References

- Anderson, J., Lampl, I., Reichova, I., Carandini, M., and Ferster, D. (2000). Stimulus dependence of two-state fluctuations of membrane potential in cat visual cortex. *Nat. Neurosci.* 3, 617–621.
- Bennett, M.V. (2000). Seeing is relieving: electrical synapses between visualized neurons. *Nat. Neurosci.* 3, 7–9.
- Blatow, M., Rozov, A., Katona, I., Hormuzdi, S.G., Meyer, A.H., Whittington, M.A., Caputi, A., and Monyer, H. (2003). A novel network of multipolar bursting interneurons generates theta frequency oscillations in neocortex. *Neuron* 38, 805–817.
- Cowan, R.L., and Wilson, C.J. (1994). Firing patterns and axonal projections of single corticostriatal neurons in the rat medial agranular cortex. *J. Neurophysiol.* 71, 17–32.
- Chapack, S., Mertz, J., Beaurepaire, E., Moreaux, L., and Delaney, K. (2001). Odor-evoked calcium signals in dendrites of rat mitral cells. *Proc. Natl. Acad. Sci. USA* 98, 1230–1234.
- Chen, B.E., Lendvai, B., Nimchinsky, E.A., Burbach, B., Fox, K., and Svoboda, K. (2000). Imaging high-resolution structure of GFP-expressing neurons in neocortex in vivo. *Learn. Mem.* 7, 433–441.
- Deans, M.R., Gibson, J.R., Sellitto, C., Connors, B.W., and Paul, D.L. (2001). Synchronous activity of inhibitory networks in neocortex requires electrical synapses containing connexin36. *Neuron* 16, 477–485.
- Denk, W., and Svoboda, K. (1997). Photon upmanship: why multiphoton imaging is more than a gimmick. *Neuron* 18, 351–357.
- Denk, W., Strickler, J.H., and Webb, W.W. (1990). Two-photon laser scanning fluorescence microscopy. *Science* 248, 73–76.
- Denk, W., Delaney, K.R., Gelperin, A., Kleinfeld, D., Strowbridge, B.W., Tank, D.W., and Yuste, R. (1994). Anatomical and functional imaging of neurons using 2-photon laser scanning microscopy. *J. Neurosci. Methods* 54, 151–162.
- Dermietzel, R., and Spray, D.C. (1993). Gap junctions in the brain: where, what type, how many and why? *Trends Neurosci.* 16, 186–192.
- Destexhe, A., and Pare, D. (1999). Impact of network activity on the integrative properties of neocortical pyramidal neurons in vivo. *J. Neurophysiol.* 81, 1531–1547.
- Eccles, J.C. (1957). *The Physiology of Nerve Cells* (Baltimore: Johns Hopkins Press).
- Fischer, F., Stegen, C.F., Koetzner, C.A., and Masters, P.S. (1998). Construction of a mouse hepatitis virus recombinant expressing a foreign gene. *Adv. Exp. Med. Biol.* 440, 291–295.
- Furshpan, E.J., and Potter, D.D. (1959). Transmission at the giant motor synapses of the crayfish. *J. Physiol.* 145, 289–325.

- Galarreta, M., and Hestrin, S. (1999). A network of fast-spiking cells in the neocortex connected by electrical synapses. *Nature* 402, 72–75.
- Galarreta, M., and Hestrin, S. (2001). Electrical synapses between GABA-releasing interneurons. *Nat. Rev. Neurosci.* 2, 425–433.
- Galarreta, M., and Hestrin, S. (2002). Electrical and chemical synapses among parvalbumin fast-spiking GABAergic interneurons in adult mouse neocortex. *Proc. Natl. Acad. Sci. USA* 99, 12438–12443.
- Gibson, J.R., Beierlein, M., and Connors, B.W. (1999). Two networks of electrically coupled inhibitory neurons in neocortex. *Nature* 402, 75–79.
- Hamill, O.P., Marty, A., Neher, A., Sakmann, B., and Sigworth, F.J. (1981). Improved patch-clamp techniques for high-resolution current recording from cells and cell-free membrane patches. *Pflügers Arch.* 391, 85–100.
- Helmchen, F., Svoboda, K., Denk, W., and Tank, D.W. (1999). *In vivo* dendritic calcium dynamics in deep-layer cortical pyramidal neurons. *Nat. Neurosci.* 2, 989–996.
- Helmchen, F., Fee, M.S., Tank, D.W., and Denk, W. (2001). A miniature head-mounted two-photon microscope. High-resolution brain imaging in freely moving animals. *Neuron* 31, 903–912.
- Hormuzdi, S.G., Pais, I., LeBeau, F.E., Towers, S.K., Rozov, A., Buhl, E.H., Whittington, M.A., and Monyer, H. (2001). Impaired electrical signaling disrupts gamma frequency oscillations in connexin 36-deficient mice. *Neuron* 31, 487–495.
- Jagadeesh, B., Wheat, H.S., and Ferster, D. (1993). Linearity of summation of synaptic potentials underlying direction selectivity in simple cells of the cat visual cortex. *Science* 262, 1901–1904.
- Kamondi, A., Acsády, L., and Buzsáki, G. (1998). Dendritic spikes are enhanced by cooperative network activity in the intact hippocampus. *J. Neurosci.* 18, 3919–3928.
- Kasper, E.M., Larkman, A.U., Lubke, J., and Blakemore, C. (1994). Pyramidal neurons in layer 5 of the rat visual cortex. I. Correlation among cell morphology, intrinsic electrophysiological properties, and axon targets. *J. Comp. Neurol.* 339, 459–474.
- Lundström, K. (2001). Alphavirus vectors for gene therapy applications. *Curr. Gene Ther.* 1, 19–29.
- MacVicar, B.A., and Dudek, F.E. (1981). Electrotonic coupling between pyramidal cells: a direct demonstration in rat hippocampal slices. *Science* 213, 782–785.
- Mainen, Z.F., Malenka, M., Shi, S.H., Hayashi, Y., Malinow, R., and Svoboda, K. (1999). Two-photon imaging in living brain slices. *Methods* 18, 231–239.
- Margrie, T.W., and Schaefer, A.T. (2003). Theta oscillation coupled spike latencies yield computational vigour in a mammalian sensory system. *J. Physiol.* 546, 363–374.
- Margrie, T.W., Brecht, M., and Sakmann, B. (2002). *In vivo*, low-resistance, whole cell recordings from neurons in the anaesthetized and awake mammalian brain. *Pflügers Arch.* 444, 491–498.
- Mason, A., and Larkman, A. (1990). Correlations between morphology and electrophysiology of pyramidal neurons in slices of rat visual cortex. II Electrophysiology. *J. Neurosci.* 10, 1415–1425.
- Masters, B.R. (1996). *Selected Papers on Confocal Microscopy* (Bellingham: SPIE Optical Engineering Press).
- Meyer, A.H., Katona, I., Biatow, M., Rozov, A., and Monyer, H. (2002). *In vivo* labeling of parvalbumin-positive interneurons and analysis of electrical coupling in identified neurons. *J. Neurosci.* 22, 7055–7064.
- Nelson, S., Toth, L., Sheth, B., and Sur, M. (1994). Orientation selectivity of cortical neurons during intracellular blockage of inhibition. *Science* 265, 774–777.
- Oheim, M., Beaupaire, E., Chaigneau, E., Mertz, J., and Charpak, S. (2001). Two-photon microscopy in brain tissue: parameters influencing the imaging depth. *J. Neurosci. Methods* 111, 29–37.
- Okabe, S., Kim, H.D., Miwa, A., Kuriu, T., and Okado, H. (1999). Continual remodeling of postsynaptic density and its regulation by synaptic activity. *Nat. Neurosci.* 2, 804–811.
- Pettit, D.L., Koothán, T., Liao, D., and Malinow, R. (1995). Vaccinia virus transfection of hippocampal slice neurons. *Neuron* 14, 685–688.
- Pines, J. (1995). GFP in mammalian cells. *Trends Genet.* 11, 326–327.
- Sanchez-Vives, M., and McCormick, D. (2000). Cellular and network mechanisms of rhythmic recurrent activity in neocortex. *Nat. Neurosci.* 3, 1027–1034.
- Schrader, M., Hofmann, U.G., and Hell, S.W. (1998). Ultrathin fluorescent layers for monitoring the axial resolution in confocal and two-photon fluorescence microscopy. *J. Microsc.* 191, 135–140.
- Shi, S.H., Hayashi, Y., Petralia, R.S., Zaman, S.H., Wenthold, R.J., Svoboda, K., and Malinow, R. (1999). Rapid spine delivery and redistribution of AMPA receptors after synaptic NMDA receptor activation. *Science* 284, 1811–1816.
- Shi, S., Hayashi, Y., Esteban, J.A., and Malinow, R. (2001). Subunit-specific rules governing AMPA receptor trafficking to synapses in hippocampal pyramidal neurons. *Cell* 105, 331–343.
- Shu, Y., Hasenstaub, A., and McCormick, D.A. (2003). Turning on and off recurrent balanced cortical activity. *Nature* 423, 288–293.
- Steriade, M., Nunez, A., and Amzica, F.A. (1993). A novel slow (<1 Hz) oscillation of neocortical neurons in vivo: depolarizing and hyperpolarizing components. *J. Neurosci.* 13, 3252–3265.
- Stern, E.A., Maravall, M., and Svoboda, K. (2001). Rapid development and plasticity of layer 2/3 maps in rat barrel cortex in vivo. *Neuron* 31, 305–315.
- Stosiek, C., Garaschuk, O., Holthoff, K., and Konnerth, A. (2003). *In vivo* two-photon calcium imaging of neuronal networks. *Proc. Natl. Acad. Sci. USA* 100, 7319–7324.
- Svoboda, K., Denk, W., Kleinfeld, D., and Tank, D.W. (1997). *In vivo* dendritic calcium dynamics in neocortical pyramidal neurons. *Nature* 385, 161–165.
- Svoboda, K., Helmchen, F., Denk, W., and Tank, D.W. (1999). Spread of dendritic excitation in layer 2/3 pyramidal neurons in rat barrel cortex *in vivo*. *Nat. Neurosci.* 2, 65–73.
- Takada, T., Iida, K., Awaji, T., Itoh, K., Takahashi, R., Shibui, A., Yoshida, K., Sugano, S., and Tsujimoto, G. (1997). Selective production of transgenic mice using green fluorescent protein as a marker. *Nat. Biotechnol.* 15, 458–461.
- Tamas, G., Buhl, E.H., Lorincz, A., and Somogyi, P. (2000). Proximally targeted GABAergic synapses and gap junctions synchronize cortical interneurons. *Nat. Neurosci.* 3, 366–371.
- Taylor, C.P., and Dudek, F.E. (1982). A physiological test for electrotonic coupling between CA1 pyramidal cells in rat hippocampal slices. *Brain Res.* 235, 351–357.
- Theer, P., Hasan, M.T., and Denk, W. (2003). Two-photon imaging to a depth of 1000 μm in living brains by use of a Ti:Al₂O₃ regenerative amplifier. *Opt. Lett.* 28, 1022–1024.
- Vigmond, E.J., Perez Velazquez, J.L., Valiante, T.A., Bardakjian, B.L., and Carlen, P.L. (1997). Mechanisms of electrical coupling between pyramidal cells. *J. Neurophysiol.* 78, 3107–3116.
- Watanabe, A. (1958). The interaction of electrical coupling among neurons of lobster cardiac ganglion. *Jap. J. Physiol.* 8, 305–318.
- Zhu, J.J., and Connors, B.W. (1999). Intrinsic firing patterns and whisker-evoked synaptic responses of neurons in the rat barrel cortex. *J. Neurophysiol.* 81, 1171–1183.